K*(892) meson production in Au+Au at $\sqrt{s_{NN}} = 200$ GeV

S. Antsupov[1], Ya.Berdnikov[1], D.Kotov[1], D.Larionova[1] for the PHENIX collaboration

[1]Peter the Great St.Petersburg Polytechnic University

October 25, 2024

We acknowledge support from Russian Ministry of Education and Science, state assignment for fundamental research (code FSEG-2024-0033)

A Physics Experiment at RHIC

Introduction

Quark-gluon plasma (QGP) is an exotic state of matter in which quarks and gluons are not bound into hadrons.

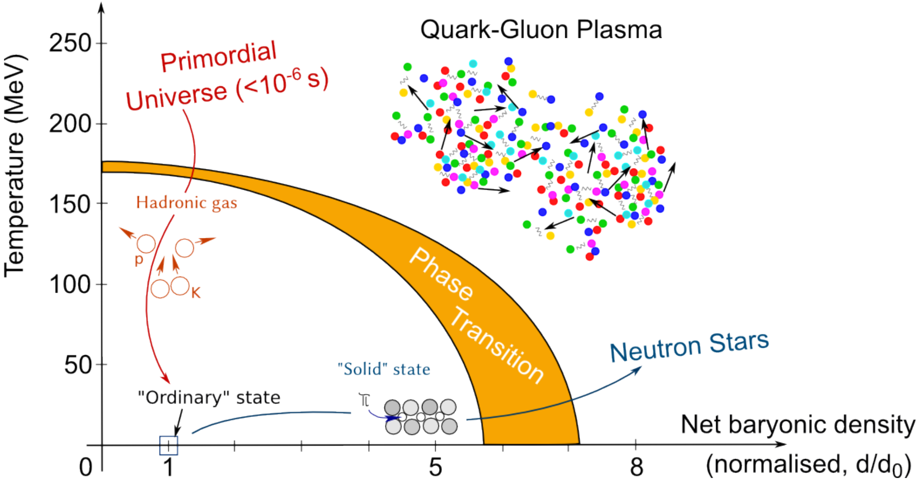

Introduction

We expect to detect the following QGP observables in our work:

- Strangeness enhancement - enhanced production of strange quarks.
- Jet quenching - energy loss of partons that constitute high energy jets.

$K^{*0}(892)$ (or $K^{*}(892)$ for this report) is a strange meson (it contains a strange quark).
Lifetime $\tau \approx 1.3 \cdot 10^{-23}$ s
In our work we observe $K^{*}(892)$ with the use of the decay mode
$K^{*}(892) \rightarrow K^{\pm}\pi^{\mp}$

Analysis workflow

1. Extraction of charged hadrons from the raw data from PHENIX experiment.
2. Formation of invariant mass distribution from extracted charged hadrons and extraction of the signal of $K^*(892)$.
3. Estimation of $K^*(892)$ reconstruction efficiency using Monte-Carlo (MC).
4. Estimation of $K^*(892)$ invariant p_T spectra, R_{AB}, R_{CP}.

Experimental apparatus

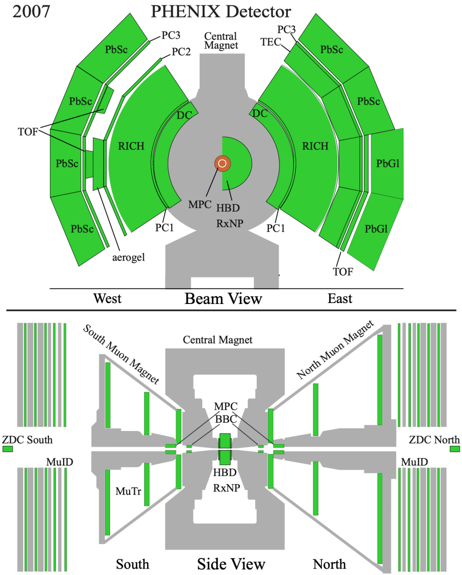

$K^*(892)$ signal extraction

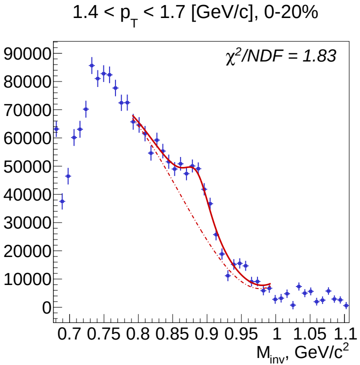

(a) $K^{\pm}\pi^{\pm}$ invariant mass distribution in 0-20% centrality class in $1.4 < p_T < 1.7$ range

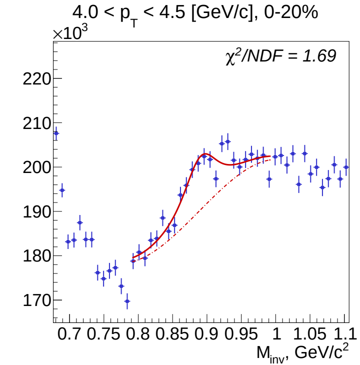

(b) $K^{\pm}\pi^{\pm}$ invariant mass distribution in 0-20% centrality class in $4.0 < p_T < 4.5$ range

- Red solid line - foreground (Relativistic Breit-Wigner) + background approximation
- Red dashed line - background approximation

$K^*(892)$ invariant p_T spectra estimation

Reconstruction efficiecny was estimated using Monte-Calro (MC) with the following formula:

$$\epsilon = \frac{N_{reconstructed}}{N_{generated}} \quad (1)$$

Where

- $N_{generated}$ - number of generated $K^*(892)$ particles in MC,
- $N_{reconstructed}$ - number of reconstructed $K^*(892)$ particles in MC.

We then estimated the $K^*(892)$ invariant p_T spectra with the use of the following formula:

$$\frac{1}{2\pi p_T}\frac{d^2N}{dydp_T} = \frac{1}{2\pi p_T \epsilon}\frac{d^2Y_{raw}}{dydp_T} \quad (2)$$

Where

- Y_{raw} - raw yield of $K^*(892)$ in the experiment,
- y - rapidity.

$K^*(892)$ invariant p_T spectra

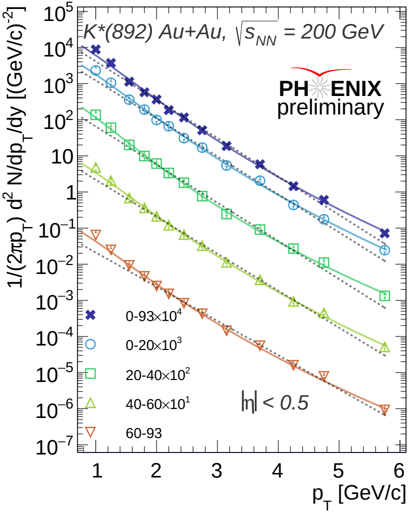

Figure: $K^*(892)$ invariant p_T spectra in Au+Au at $\sqrt{s_{NN}} = 200$ GeV

The invariant p_T distribution of $K^*(892)$ was measured at $0.9 < p_T < 6.5$ GeV/c and for 0-20%, 20-40%, 40-60%, 60-93%, MB centrality classes.

- Dashed lines - exponential fits
- Solid lines - Levy fits

Nuclear modification factors R_{AA} estimation

We estimated $K^*(892)$ R_{AA} with the use of the following formula:

$$R_{AB} = \frac{1}{N_{coll}} \frac{1/2\pi p_T \ d^2N_{AB}/dydp_T}{1/2\pi p_T \ d^2N_{pp}/dydp_T} \quad (3)$$

Where

- N_{coll} - average number of nucleon-nucleon collisions in A+B collision,
- $1/2\pi p_T \ d^2N_{AB}/dydp_T$ - invariant p_T spectra in A+B collision,
- $1/2\pi p_T \ d^2N_{pp}/dydp_T$ - invariant p_T spectra in p+p collision.

Nuclear modification factors R_{AA}

$K^*(892)$ R_{AA} were measured at $0.9 < p_T < 6.5$ GeV/c and for 0-20%, 20-40%, 40-60%, 60-93%, MB centrality classes.

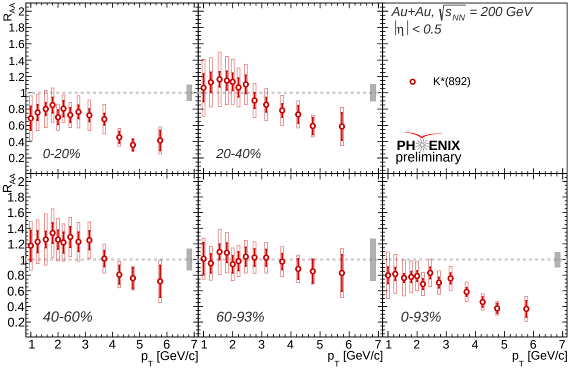

Figure: $K^*(892)$ R_{AA} in Au+Au at $\sqrt{s_{NN}} = 200$ GeV

- Error bars represent statistical uncertainties
- Colored empty boxes represent systematic uncertainties
- Filled gray boxes on the right of each picture represent N_{coll} uncertainties

Nuclear modification factors R_{AA}

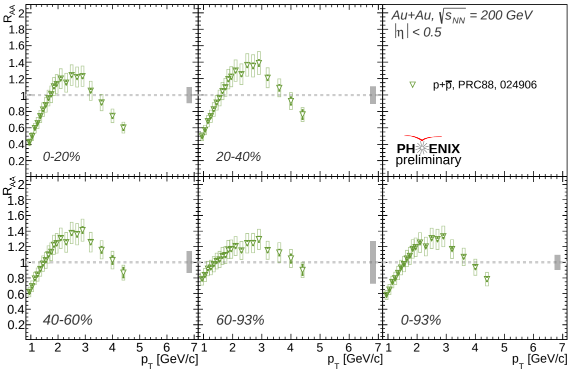

Figure: $p + \bar{p}$ R_{AB} in Au+Au at $\sqrt{s_{NN}} = 200$ GeV

- Error bars represent statistical uncertainties
- Colored empty boxes represent systematic uncertainties
- Filled gray boxes on the right of each picture represent N_{coll} uncertainties

Nuclear modification factors R_{AA}

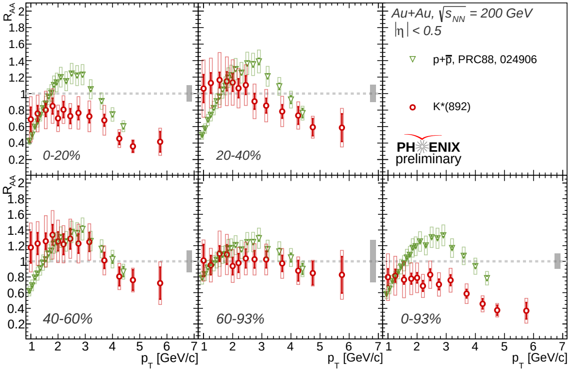

Figure: $p + \bar{p}$, $K^*(892)$ R_{AB} in Au+Au at $\sqrt{s_{NN}} = 200$ GeV

- Error bars represent statistical uncertainties
- Colored empty boxes represent systematic uncertainties
- Filled gray boxes on the right of each picture represent N_{coll} uncertainties

Nuclear modification factors R_{AA}

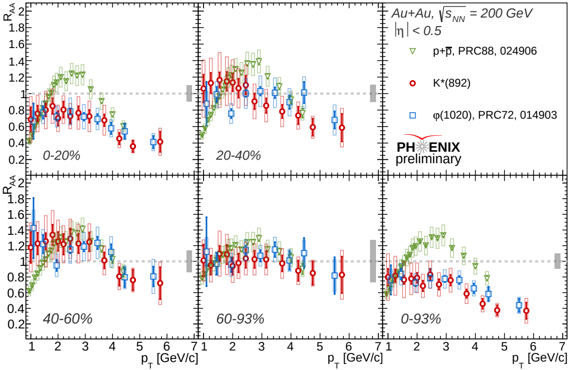

Figure: $p + \bar{p}$, $K^*(892)$, $\varphi(1020)$ R_{AB} in Au+Au at $\sqrt{s_{NN}} = 200$ GeV

- Error bars represent statistical uncertainties
- Colored empty boxes represent systematic uncertainties
- Filled gray boxes on the right of each picture represent N_{coll} uncertainties

Nuclear modification factors R_{AA}

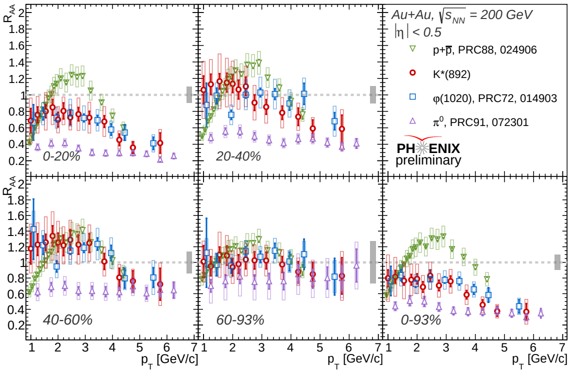

Figure: $p + \bar{p}$, $K^*(892)$, $\varphi(1020)$ and π^0 R_{AB} in Au+Au at $\sqrt{s_{NN}} = 200$ GeV

- Error bars represent statistical uncertainties
- Colored empty boxes represent systematic uncertainties
- Filled gray boxes on the right of each picture represent N_{coll} uncertainties

Nuclear modification factors R_{CP} estimation

We estimated $K^*(892)$ R_{AA} with the use of the following formula:

$$R_{CP} = \frac{N_{coll}^{peripheral}}{N_{coll}^{central}} \frac{1/2\pi p_T \ d^2 N_{AB}^{central}/dydp_T}{1/2\pi p_T \ d^2 N_{AB}^{peripheral}/dydp_T} \quad (4)$$

Where

- $N_{coll}^{central}$, $N_{coll}^{peripheral}$ - average number of nucleon-nucleon collisions in A+B collision in central and peripheral centrality classes respectively,
- $1/2\pi p_T \ d^2 N_{AB}^{central}/dydp_T$, $1/2\pi p_T \ d^2 N_{AB}^{peripheral}/dydp_T$ - invariant p_T spectra in A+B collision in central and peripheral centrality classes respectively.

Nuclear modification factors R_{CP}

$K^*(892)$ R_{CP} were measured at $0.9 < p_T < 6.5$ GeV/c for 0-20%/40-60% and 0-20%/60-93% centrality classes ratios.

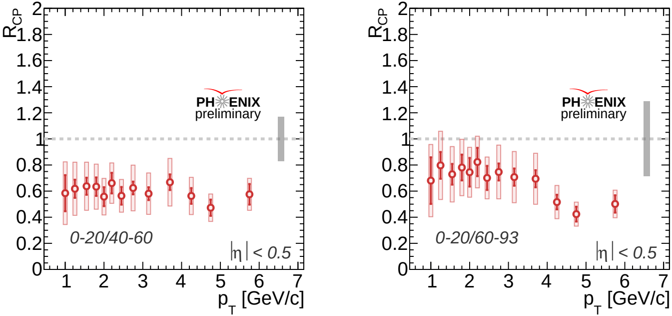

Figure: $K^*(892)$ R_{CP} in Au+Au at $\sqrt{s_{NN}} = 200$ GeV

- Error bars represent statistical uncertainties
- Colored empty boxes represent systematic uncertainties
- Filled gray boxes on the right of each picture represent N_{coll} uncertainties

Nuclear modification factors R_{CP}

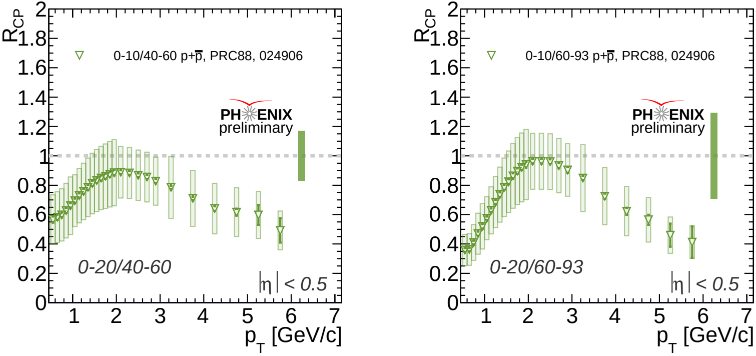

Figure: $p + \bar{p}$ R_{CP} in Au+Au at $\sqrt{s_{NN}} = 200$ GeV

- Error bars represent statistical uncertainties
- Colored empty boxes represent systematic uncertainties
- Filled colored boxes on the right of each picture represent N_{coll} uncertainties of the corresponding particles with the same color of the marker.

Nuclear modification factors R_{CP}

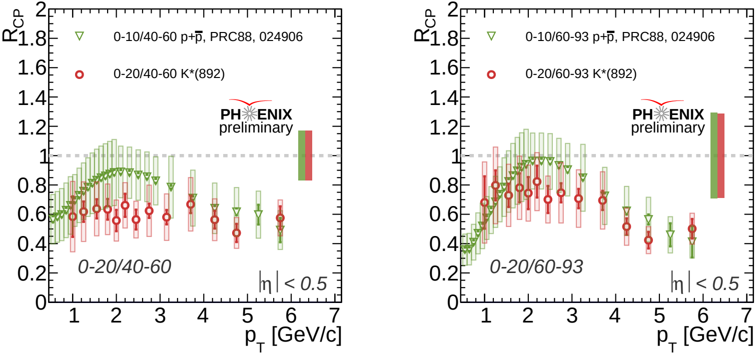

Figure: $p + \bar{p}$, $K^*(892)$ R_{CP} in Au+Au at $\sqrt{s_{NN}} = 200$ GeV

- Error bars represent statistical uncertainties
- Colored empty boxes represent systematic uncertainties
- Filled colored boxes on the right of each picture represent N_{coll} uncertainties of the corresponding particles with the same color of the marker.

Nuclear modification factors R_{CP}

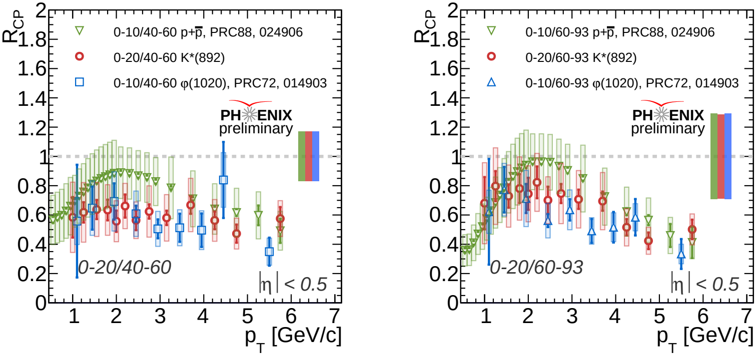

Figure: $p + \bar{p}$, $K^*(892)$, $\varphi(1020)$ R_{CP} in Au+Au at $\sqrt{s_{NN}} = 200$ GeV

- Error bars represent statistical uncertainties
- Colored empty boxes represent systematic uncertainties
- Filled colored boxes on the right of each picture represent N_{coll} uncertainties of the corresponding particles with the same color of the marker.

Nuclear modification factors R_{CP}

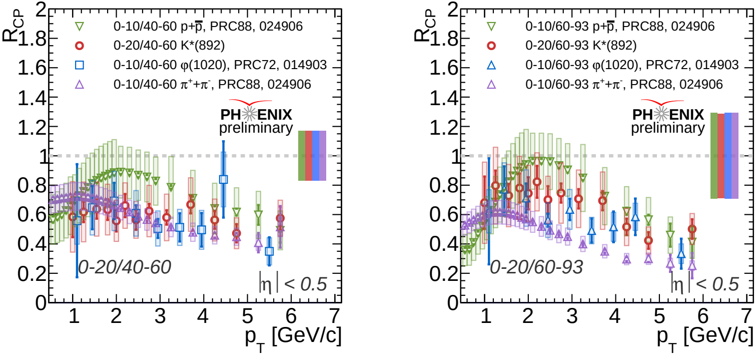

Figure: $p + \bar{p}$, $K^*(892)$, $\varphi(1020)$ and π^0, and R_{CP} in Au+Au at $\sqrt{s_{NN}} = 200$ GeV

- Error bars represent statistical uncertainties
- Colored empty boxes represent systematic uncertainties
- Filled colored boxes on the right of each picture represent N_{coll} uncertainties of the corresponding particles with the same color of the marker.

Conclusions

- We observed that values of R_{AA} and R_{CP} for $K^*(892)$ and $\varphi(1020)$ are close and are mostly within uncertainties of each other thus the impact of effects of suppression and enhancement are similar for both $K^*(892)$ and $\varphi(1020)$.
- We observed the difference of R_{AA} and R_{CP} between $K^*(892)$ and $p + \bar{p}$ which can be explained by the recombination models. This is because recombination models predict higher baryon yield than meson yield.
- We observed the difference of R_{AB} and R_{CP} between $K^*(892)$ and π^0 which can also be explained by the recombination models. Recombination models predict thermal over shower partons recombination dominance for $K^*(892)$ and $\varphi(1020)$ up to 6 GeV/c in p_T due to the strangeness enhancement while the same dominance for π^0 only spans up to 3 GeV/c.

Thank you for your attention!

Backup: previous measurements (STAR) of $K^*(892)$ in Au+Au at $\sqrt{s_{NN}} = 200$ GeV

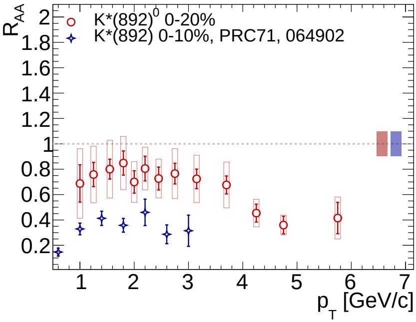

Our result of $K^*(892)$ R_{AA} in 0-20% centrality class and STAR result of $K^*(892)$ R_{AA} in 0-10% centrality class in Au+Au @ $\sqrt{s_{NN}} = 200$ GeV

Our values are almost 2 times bigger than STAR values

Possible explanation:
STAR employs both $K^{*0}(892)$ and $K^{*\pm}(892)$ for the calculation of invariant p_T spectra and R_{AA}

Backup: Explanation of STAR vs PHENIX $K^*(892)$ discrepancy

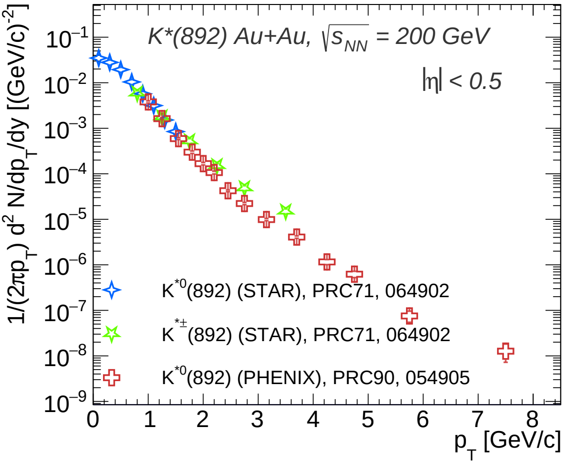

PHENIX vs STAR measurements of $K^*(892)$ invariant p_T spectra in p+p at $\sqrt{s_{NN}} = 200$ GeV

Backup: Comparison of $K^*(892)$ R_{AA} on PHENIX vs estimated R_{AA} of $K^*(892)$ on STAR

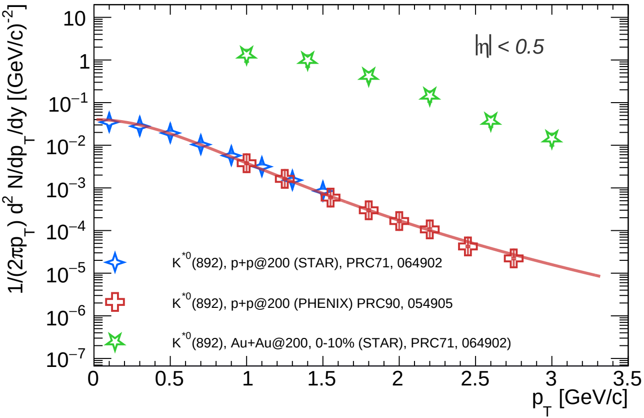

Invariant p_T spectra of $K^*(892)$ in p+p collisions at $\sqrt{s_{NN}} = 200$ GeV from PHENIX and STAR.

Backup: Comparison of $K^*(892)$ R_{AA} on PHENIX vs estimated R_{AA} of $K^*(892)$ on STAR

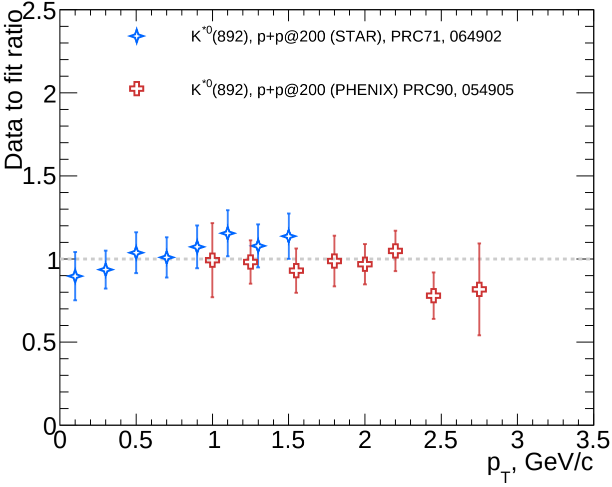

Ratio of merged invariant p_T spectra of $K^*(892)$ in p+p collisions at $\sqrt{s_{NN}} = 200$ GeV from PHENIX and STAR to it's Levy approximation.

Backup: Comparison of neutral $K^*(892)$ R_{AA} on PHENIX vs estimated R_{AA} of neutral $K^*(892)$ on STAR

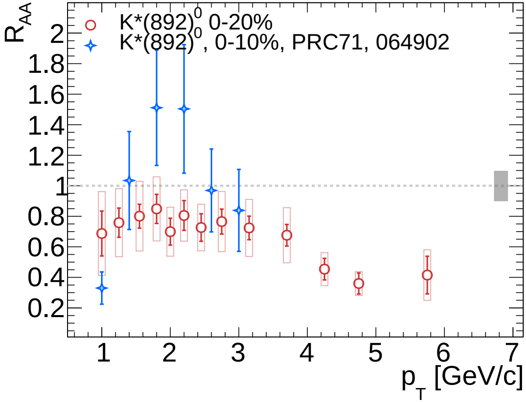

Figure: $K^*(892)$ R_{AA} in Au+Au at $\sqrt{s_{NN}} = 200$ GeV

- Error bars represent statistical uncertainties
- Colored empty boxes represent systematic uncertainties
- Filled gray boxes on the right of each picture represent N_{coll} uncertainties